

Hydraulic flow tests of APWR reactor internals for safety analysis

Tadashi Morii*

Nuclear Power Facility Safety Analysis Group, Safety Analysis and Evaluation Division, Japan Nuclear Energy Safety Organization, Kamiya-cho MT Building, 12F, 4-3-20 Toranomon, Minato-ku, Tokyo 105-0001, Japan

Received 3 October 2006; received in revised form 23 January 2007; accepted 11 February 2007

Abstract

A concept of radial neutron reflector of APWR brings about safety problems relevant to the flow induced vibration and thermal deformation. The CFD code has been expected to solve them by calculating pressure fluctuations of turbulent flow in the downcomer and the flow distribution into the neutron reflector. A series of hydraulic flow tests was conducted by NUPEC from 1998 to 2002 to demonstrate the new design of the neutron reflector and to obtain test data for validating the CFD code. The measured pressure fluctuations in the downcomer and their statistics were utilized for validating the specific turbulent model to be able to calculate a spectrum of pressure fluctuation such as the LES model. The measured flow rates at inlet holes of the lower core plate were utilized for validating the general turbulent model, for example, the $k-\varepsilon$ turbulent model. The calculated results with the LES model agreed well with the measured pressure fluctuations and their spectrum, but did not agree with the correlation between adjacent pressure fluctuations. On the other hand, the calculation results with the $k-\varepsilon$ turbulent model agreed well with the measured flow rates at inlet holes of the lower core plate.

© 2007 Elsevier B.V. All rights reserved.

1. Introduction

The APWR, featuring many innovative technologies for safety and economic improvement, is expected to be a future standardized PWR in Japan. One of the most important design improvements is the concept of a radial neutron reflector which replaces the baffle structures in current PWRs. This new reflector is designed to improve the reliability of the reactor structure and the efficient use of uranium resources. On the other hand, this new design brings about safety problems relevant to the flow induced vibration of reactor internals including the neutron reflector and, coolability and thermal deformation of radial reflector blocks. The CFD code has been expected to solve them by calculating pressure fluctuations of turbulent flow in a downcomer and the flow distribution into the neutron reflector through the inlet holes.

A series of hydraulic flow tests was conducted by NUPEC from 1998 to 2002 to demonstrate the new design of the neutron

reflector and to obtain test data for validating the CFD code. The test vessel was the 1/5-scaled model of the APWR reactor vessel. The test includes the flow induced vibration measurements and the flow distribution measurements.

2. Flow induced vibration measurements

A vibration of the core barrel caused by the turbulent flow in the downcomer shakes the radial reflector through the water between them (Fig. 1). When the radial reflector vibrates, it may make contact with and shake the adjacent fuel bundles and could result in fretting, and possibly rupture, of the fuel pin cladding.

2.1. Test facility and conditions

Fig. 2 shows the test facility. Measuring instruments are shown in Table 1. The tests were performed with varying flow rate and temperature of water in the following range:

- Flow rate: 60–120% of the nominal flow rate (4670 m³/h).
- Temperature: 50–150 °C.

* Tel.: +81 3 4511 1531; fax: +81 3 4511 1598.
E-mail address: morii-tadashi@jnes.go.jp.

Nomenclature

f	frequency
f_0	frequency at which non-dimensional cross spectrum decreases by 1/e
n	number of pressure measurements but neighborhood of the inlet nozzle
p_i	measured pressure of the i th pressure transducer
p'_i	turbulent fluctuation of the i th pressure transducer
p_0	common mode noise of the i th pressure transducer
\bar{p}_0	approximate value of p_0
q_i	flow rate of i th hole of the lower core plate
q_{avg}	averaged flow rate of all holes of the lower core plate
U	advective velocity in the downcomer
W_{XX}, W_{YY}	power spectrum of pressure fluctuation
W_{XY}	cross spectrum between adjacent pressure fluctuation X and Y
x', x''	locations of pressure sensors

Greek symbols

λ	correlation length
Γ_{XY}	non-dimensional cross spectrum between adjacent pressure fluctuation X and Y
Γ_0	real part of non-dimensional cross spectrum at 0 Hz

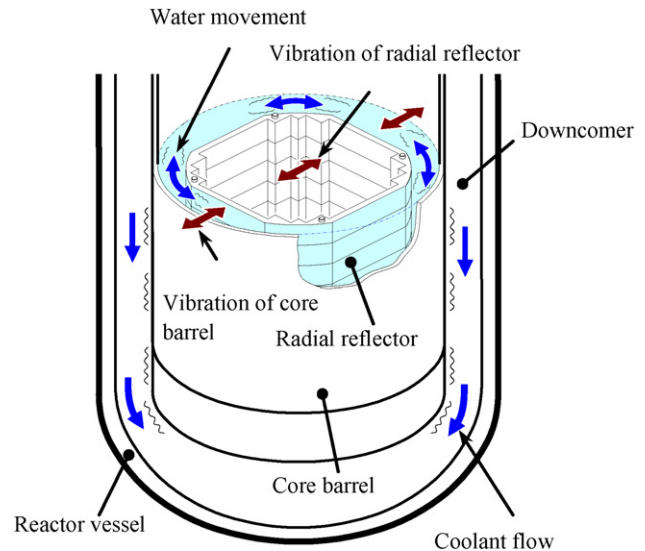


Fig. 1. Flow induced vibration of the radial reflector of APWR.

2.2. Test results

A lot of data for vibration and displacement of structures were obtained in the test, but only pressure fluctuations of water are discussed in this paper in a view of CFD code validation. Detail of measurement system of pressure fluctuation is shown

in Fig. 3. Figs. 4 and 5 show the measured time histories of pressure fluctuation at 0° and 90° (see Fig. 3) of the upper part of the downcomer under the condition of different flow rate. Fluctuation increases monotonically as flow rate increases and the fluctuation near an inlet nozzle (Fig. 5) is larger than that far from an inlet (Fig. 4). Since the measured data contains the fluctuation caused by the proper vibration of the piping and test vessel, it should be separated and subtracted from the measured data because it has no relation to turbulence. The method how to separate the signals of the common vibration from the measured data is described in Appendix A.

The correlation length can be estimated from the data of a couple of pressure transducers set as shown in Fig. 3. The non-dimensional cross spectrum Γ_{XY} between adjacent pressure

Table 1
Measuring instruments used for the flow induced vibration measurement

Location	Instrument	Measured values ^a	Number	Error (%)
1. Core barrel	Pressure transducers	Pressure fluctuation ^b	21 ^b	1.0
	Accelerometers	Acceleration	18	0.13
	Strain gauge	Strain	8	3.2
2. Neutron reflector	Pressure transducers	Pressure fluctuation	3	0.27
	Accelerometers	Acceleration	16	0.13
	Displacement meters	Displacement	2	1.0
3. Upper core plate	Force measure	Exciting force	4	1.0
4. Control rod guide tube	Strain gauge	Strain	6	3.2
5. Upper core support pole	Strain gauge	Strain	4	3.2
6. Inlet of test vessel	Thermo-couple	Temperature	1	1.0
	Pressure transducers	Water pressure	1	0.09
	Flow meter	Water flow rate	1	1.0
7. Outlet of test vessel	Pressure transducers	Water pressure	1	0.09
8. Test vessel	Accelerometers	Acceleration	6	0.09
9. Plate in lower plenum	Accelerometers	Acceleration	4	0.09

^a The sampling rate is 5.12 kHz and the sampling time is 30 s.

^b The relevant data for CFD code validation.

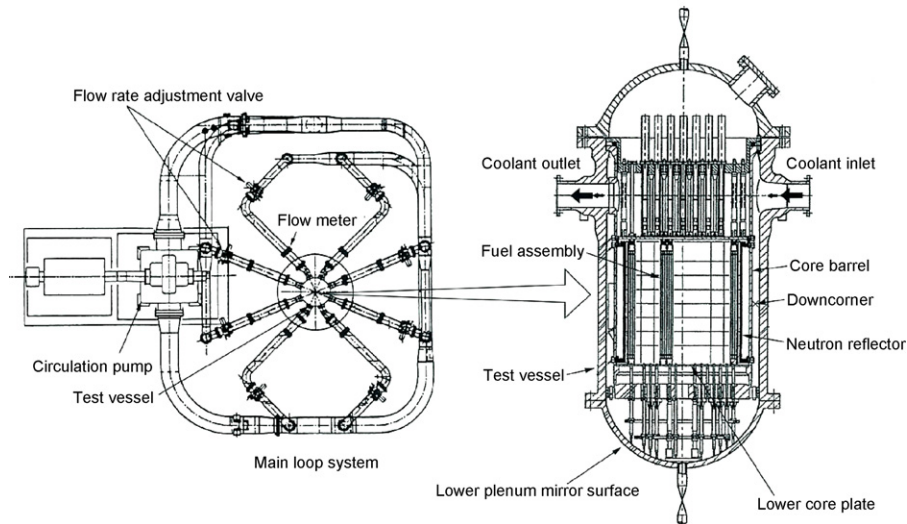


Fig. 2. Test facility of flow induced vibration test and hydraulic flow test.

fluctuation X and Y is defined by the following equation:

$$\Gamma_{XY} = \frac{W_{XY}}{\sqrt{W_{XX}}\sqrt{W_{YY}}} \quad (1)$$

Here, W_{XX} and W_{YY} are the power spectrum, W_{XY} is the cross spectrum.

Figs. 6 and 7 show the two curves of real part of the non-dimensional cross spectrum. A jagged one is calculated by Eq. (1) with two of the measured pressure fluctuations, and the other smooth one is the curve fit to the jagged line obtained by the following process. The cross spectrum consists of two different types of correlation. One is a correlation between two adjacent pressure transducers set axially, namely along flow direction and the other between transducers set circumferentially.

The axial cross spectrum oscillates and is damped as frequency increases because of phase difference corresponding to time delay between signals of two sensors set along flow. On the other hand, the circumferential cross spectrum is damped monotonically because of no clear circumferential

flow. Therefore, the evaluation method for correlation length should be distinguished between axial and circumferential directions (Au-Yang, 1980, 1999):

- Axial cross spectrum:

$$\begin{aligned} \text{Re}(\Gamma_{XY}) &= \exp\left(-\frac{|x' - x''|}{\lambda}\right) \cos\left(\frac{2\pi f |x' - x''|}{U}\right) \\ \lambda &= \frac{-|x' - x''|}{\ln(\Gamma_0) - f/f_0} \end{aligned} \quad (2)$$

- Circumferential cross spectrum:

$$\text{Re}(\Gamma_{XY}) = \exp\left(-\frac{|x' - x''|}{\lambda}\right) \quad (3)$$

Here, x' and x'' are the locations of sensors, λ the correlation length, U the advective velocity, Γ_0 the real part of non-

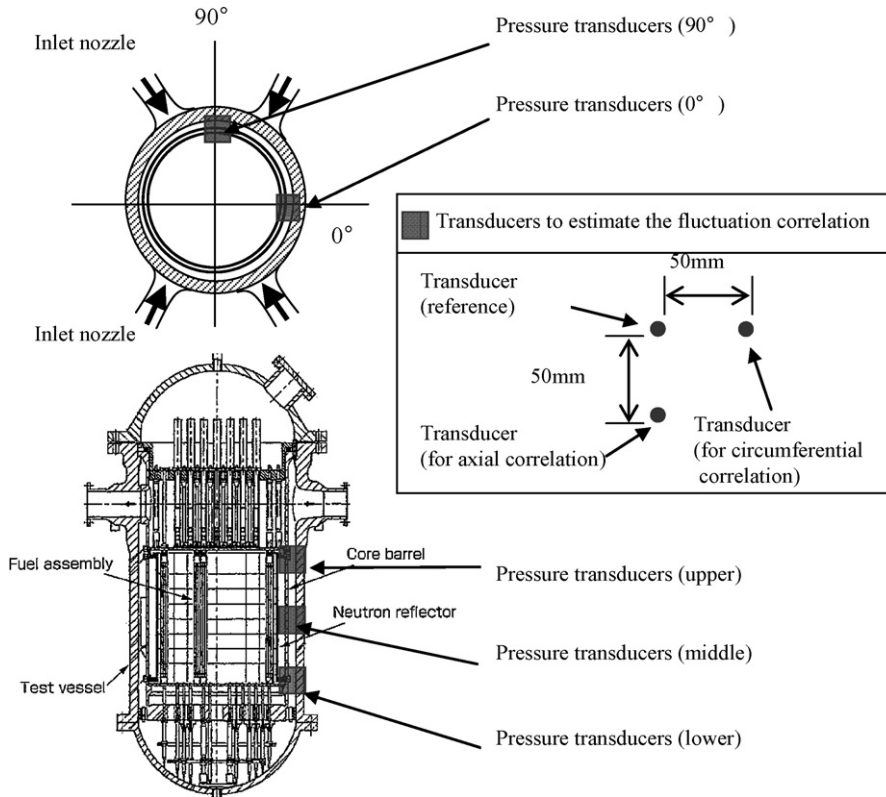


Fig. 3. Detail of pressure fluctuation measurement.

dimensional cross spectrum at 0 Hz, f the frequency, and f_0 is the frequency at which non-dimensional cross spectrum decreases by $1/e$.

Figs. 8 and 9 show the correlation length λ obtained from the smooth curve in Figs. 6 and 7 expressed by Eq. (2). The circumferential correlation length at 90° (see the second row of

figures in Fig. 8) is 0 in upper part of downcomer and increases with distance downstream from it. This is because the upper part lies in the middle of two inlet nozzles and the correlation length, therefore, becomes 0. The axial correlation length at 90° (see the first row of Fig. 8) decreases downstream from the upper part of the downcomer because axial advection in the flow field

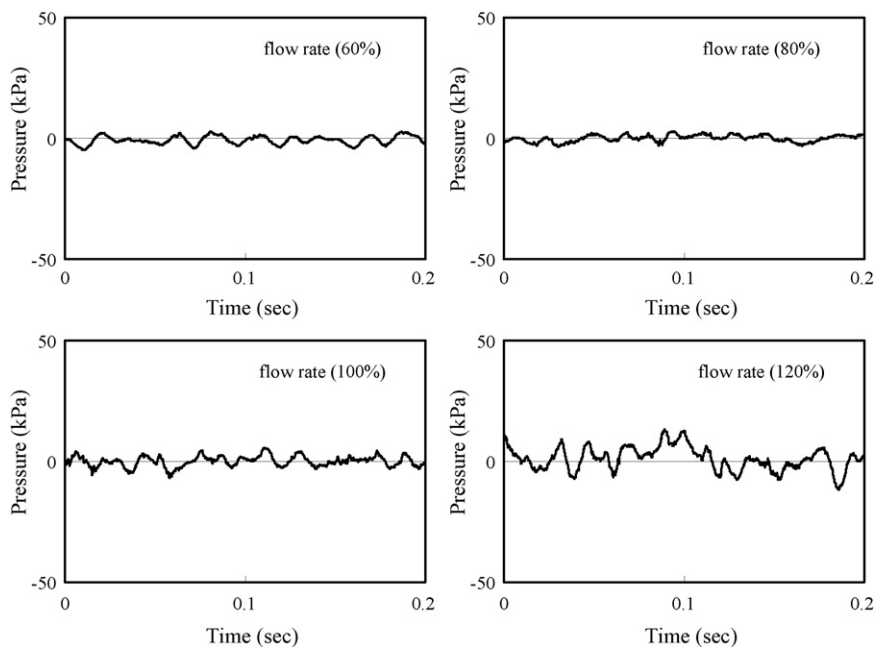


Fig. 4. Pressure fluctuation at 0° of the upper downcomer vs. flow rate (150°C).

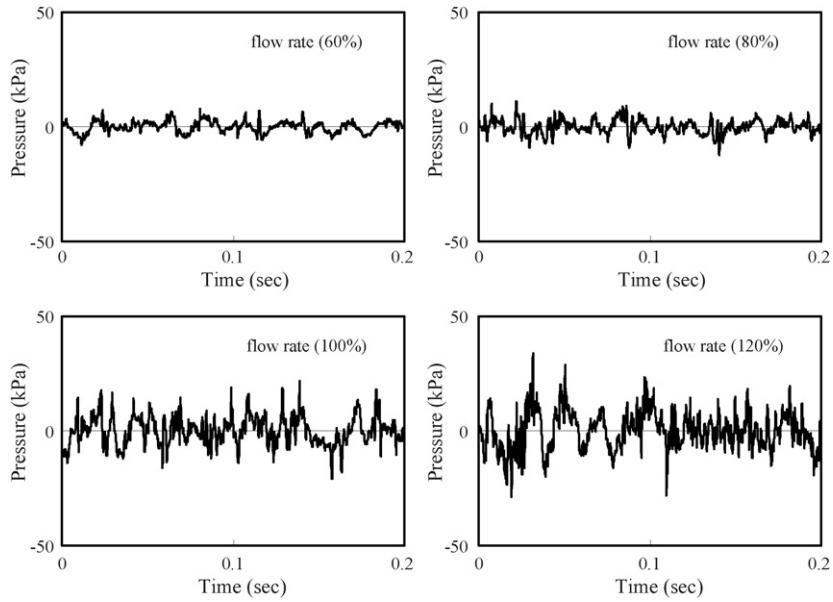


Fig. 5. Pressure fluctuation at 90° of the upper downcomer vs. flow rate (150 °C).

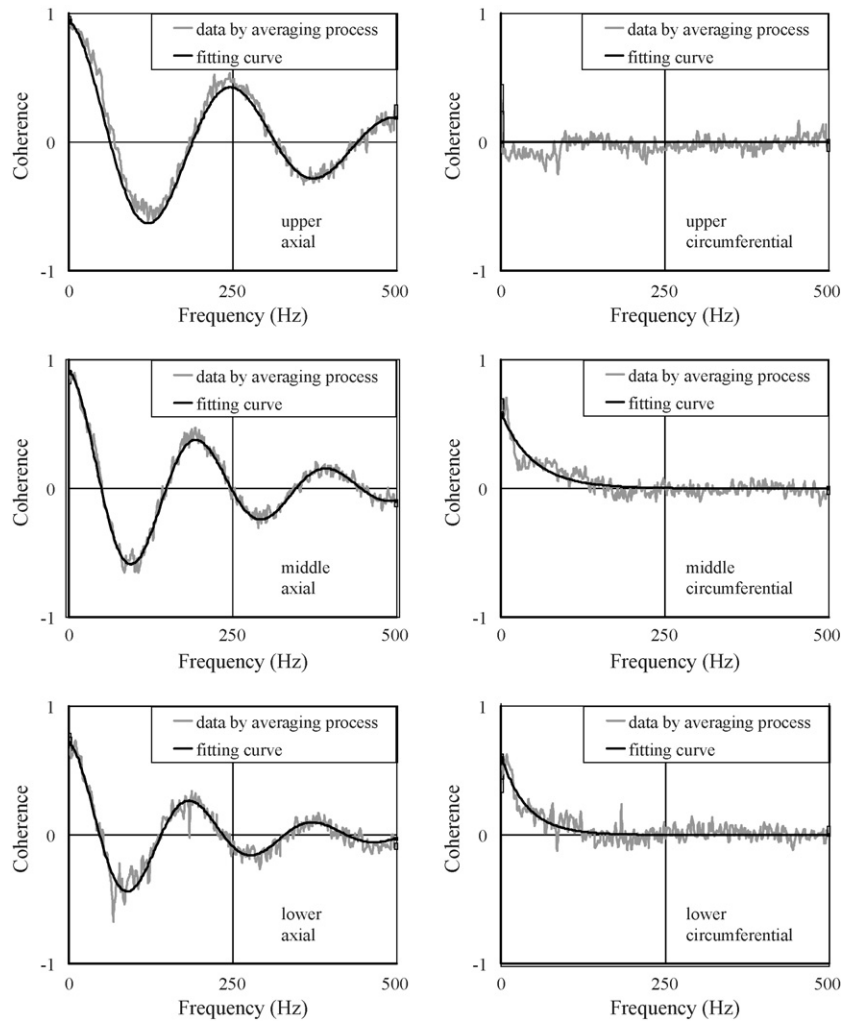


Fig. 6. Spectrums of pressure fluctuations (90°, 150 °C).

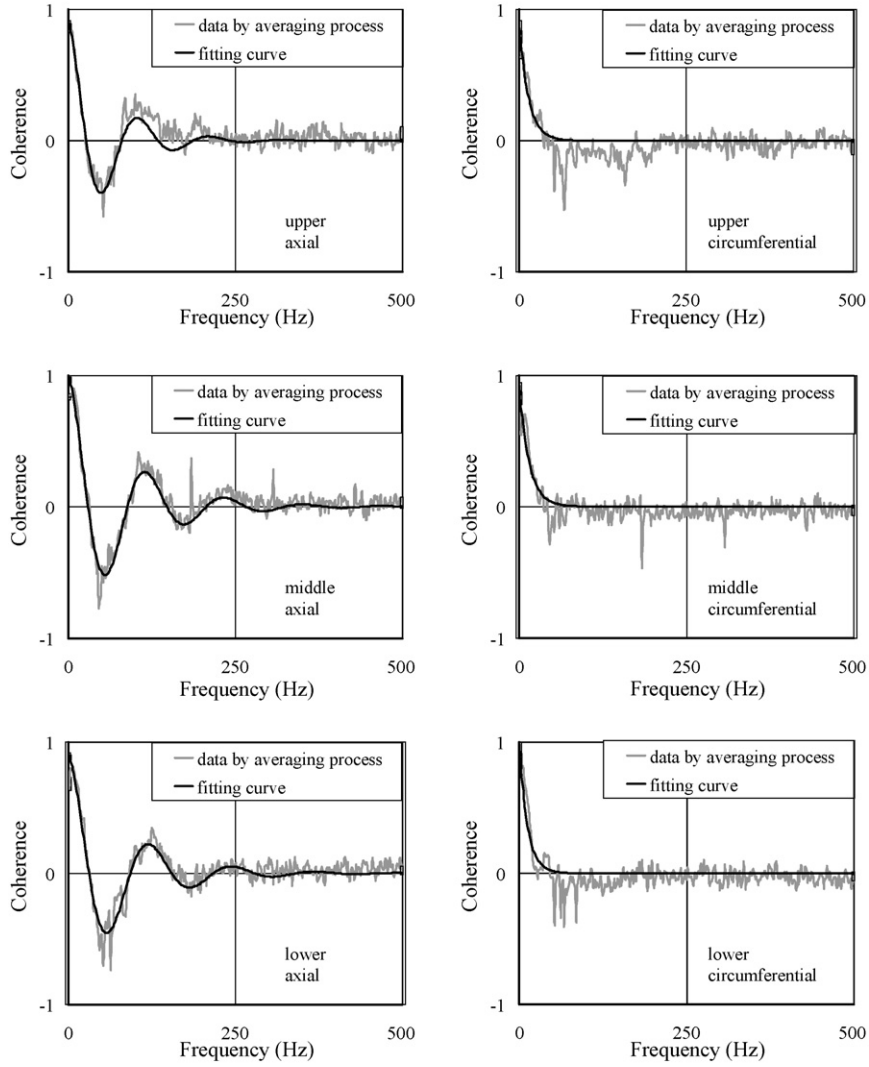


Fig. 7. Spectrums of pressure fluctuations (0°, 150 °C).

weakens in the lower part. On the other hand, the circumferential and axial correlation lengths at 0° (see Fig. 9) are almost same shape respectively without distinction of the upper and lower parts of the downcomer. This means a uniform flow field at 0° of the downcomer.

2.3. CFD calculation (Kasahara et al., 2002)

The downcomer was modelled using about 550,000 structured cells with the BFC technique shown in Fig. 10. A 3D transient turbulent flow in the downcomer was calculated by the

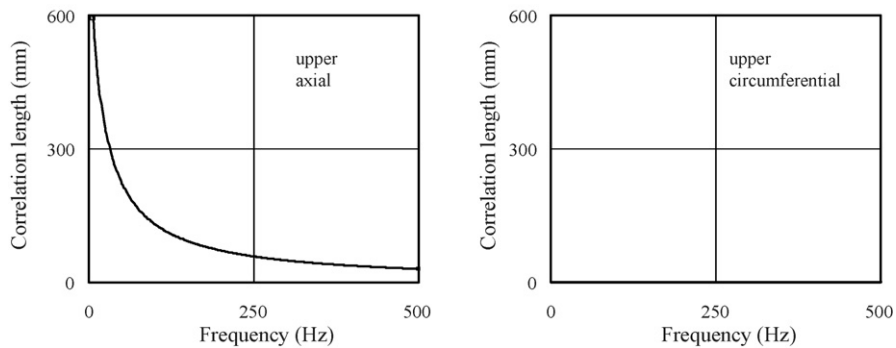


Fig. 8. Correlation length of pressure fluctuations (90°, 150 °C, 100% flow).

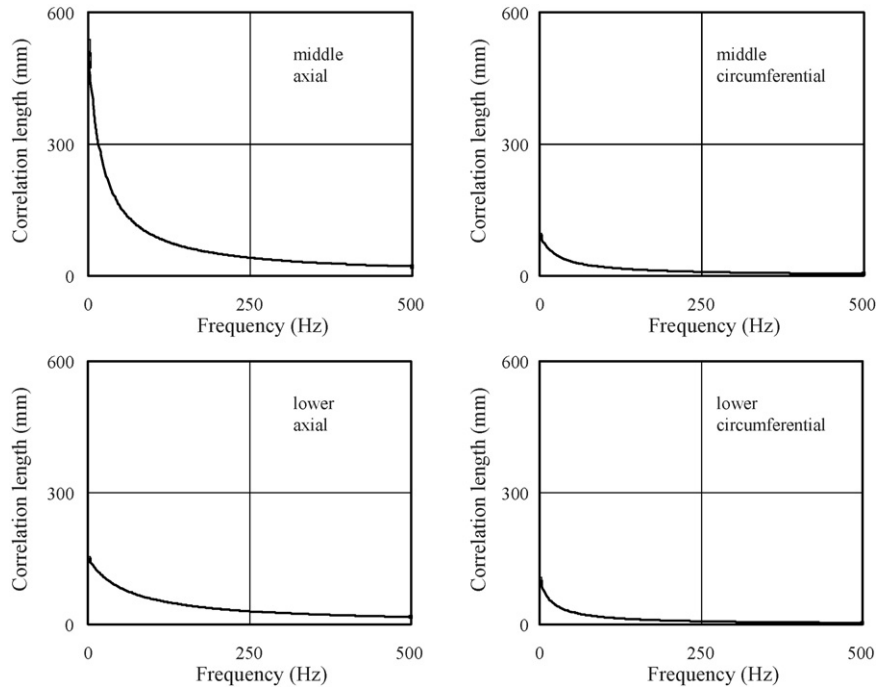


Fig. 8. (Continued).

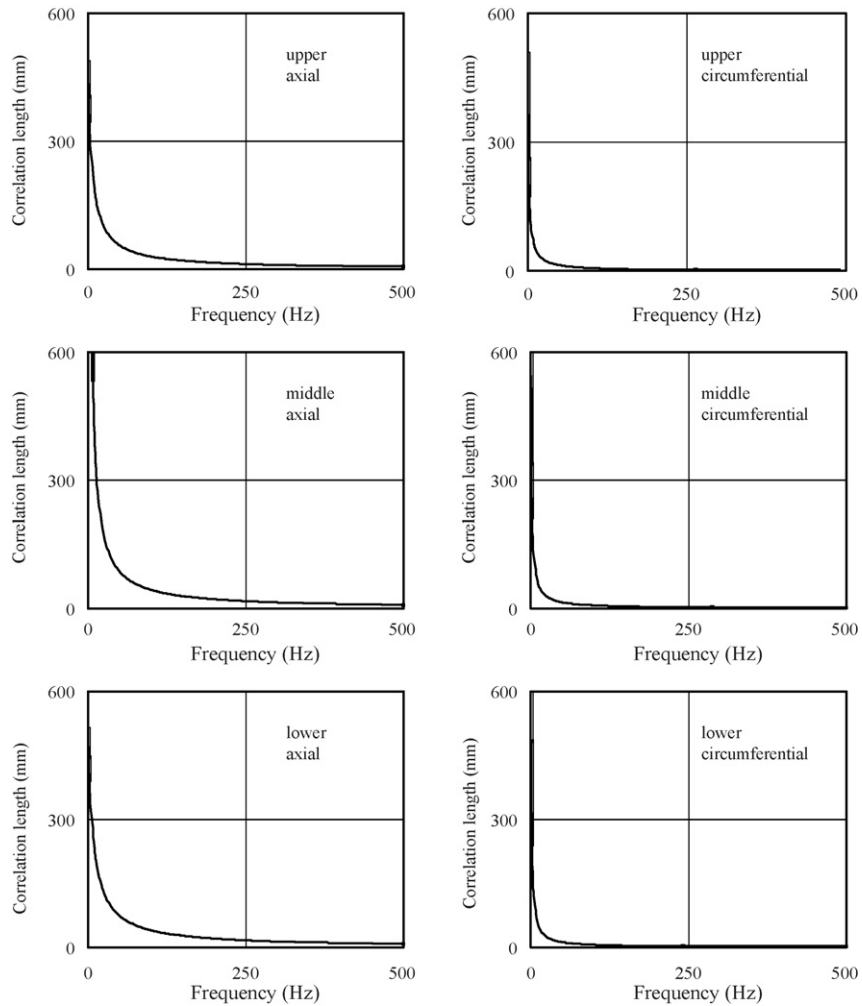


Fig. 9. Correlation length of pressure fluctuations (0°, 150 °C, 100% flow).

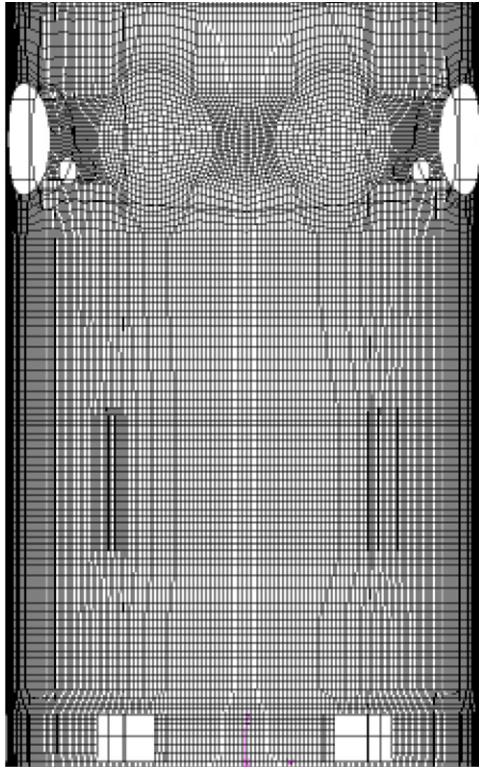


Fig. 10. Calculation grid for the downcomer of test vessel.

PLASHY code (Gavrilas et al., 2000; Morii et al., 2001a) using the LES turbulent model and a second-order upwind method (QUICK). The reason for selecting the LES model is as follows. The unsteady RANS (Reynolds-Averaged Navier Stokes) turbulent model solves the time averaged Navier Stokes equation, as against the LES solves the Navier Stokes equation with no approximation for a time behavior. The pressure fluctuation

analysis in this paper requires an ability of obtaining pressure history with high accuracy of time.

The fine zigzag line in Fig. 11 shows calculated axial cross spectrum at upper, middle and lower position in the downcomer and the bold line shows the most fitted curve to the fine zigzag line among curves expressed by Eq. (2) and agrees well with the curve in the first row of figures in Fig. 6. The calculated spectrum at upper part of downcomer can be fitted by Eq. (2) up to 400 Hz but the calculated spectrum downstream tends to be away from Eq. (2) in high frequency (above about 200 Hz). It is thought that the principal reason for discrepancy between calculated results and test data is an insufficient resolution of the calculation grids. The correct estimation of correlation of pressure fluctuations requires precise simulation of very small turbulent eddies. The behavior of an eddy can be captured by the grids, the interval of which is smaller than the size of the relevant eddy. The other reason is an insufficient simulation time. The statistics were obtained by the statistical process of the results calculated during the simulation time. In fact, the simulation time is about 0.5 s as against 30 s of measuring time of the test.

3. Flow distribution measurements

3.1. Test facility and conditions

Measuring instruments are shown in Table 2. The tests were performed with varying flow rate and temperature of water in the same range as the flow induced vibration measurements:

- Flow rate: 60–120% of the nominal flow rate (4670 m³/h).
- Temperature: 50–150 °C.

3.2. Test results

Flow rate at inlet holes of the lower core plate, pressure on lower core plate and pressure on inner surface of vessel bottom

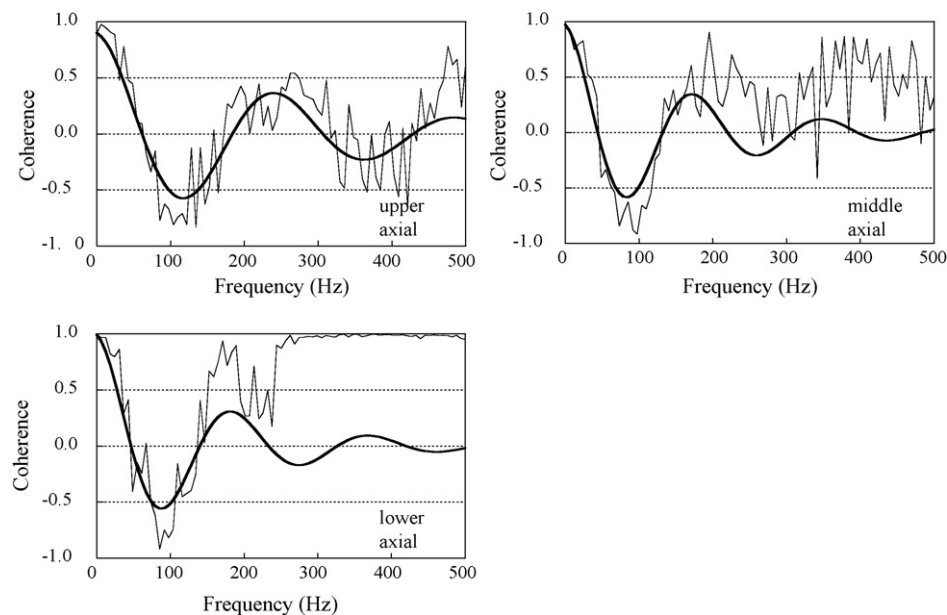


Fig. 11. Calculated results for axial cross spectrum (90°, 150 °C, 100% flow).

Table 2
Measuring instruments used for the flow distribution measurement

Location	Instrument	Measured values ^a	Number	Error (%)
1. Inlet holes of lower core plate	Pressure (difference) transducers	Flow rate ^b	40 ^b	0.12
	Pressure transducers	Pressure fluctuation	2	0.27
2. Lower core plate	Pressure transducers	Pressure ^b	40 ^b	0.27
3. Inner surface of vessel bottom	Pressure transducers	Pressure ^b	47 ^b	1.0
	Pressure transducers	Pressure fluctuation	2	1.0
4. Core inlet	Pressure transducers	Pressure loss of core	4	0.12
5. Core outlet	Pressure transducers	Pressure loss of core	4	0.12
6. Inlet of test vessel	Thermo-couple	Temperature	1	1.0
	Pressure transducers	Water pressure	1	0.29
	Flow meter	Water flow rate	1	1.0

^a The sampling rate is 5.12 kHz and the sampling time is 30 s.

^b The relevant data for CFD code validation.

in Table 2 can be used to validate the CFD code. A detailed view of measurement locations for these data is shown in Fig. 12. The flow rates at inlet holes were not measured by the flow meter, but by pressure transducers installed on both faces of the plate. The flow rate was calculated from the pressure difference between inlet and outlet of the hole.

Fig. 13 shows the measured flow rate of 40 holes on the lower core plate through which a small portion of coolant flows into the radial reflector. The *x*-axis means the location of the hole represented by an angle shown in Fig. 12 and the *y*-axis means the ratio of flow rate of each hole defined by q_i/q_{avg} and here, q_i and q_{avg} are the flow rate of the *i*th hole and the averaged flow rate of all holes, respectively. No dependency of the flow distribution on coolant flow rate and temperature can be seen from the figure. The measured pressure on the surface of the lower core plate is shown in Fig. 14. Pressure of the *y*-axis means a deviation from the averaged pressure. Pressure deviation has a dependency of the square of total coolant flow rate and little

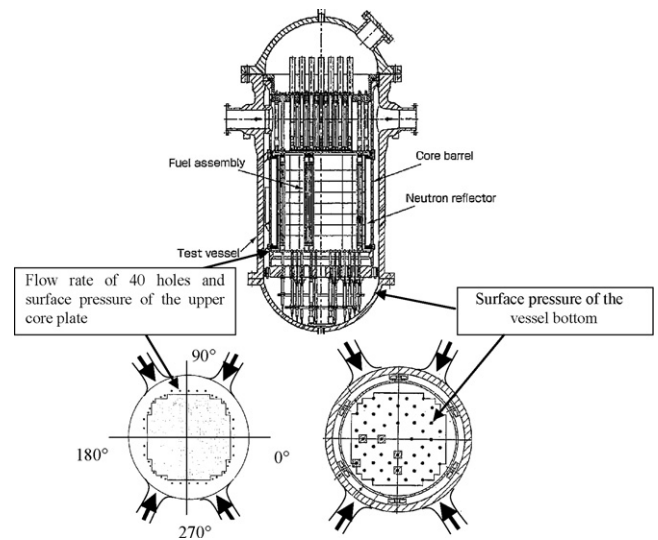


Fig. 12. Flow distribution measurement.

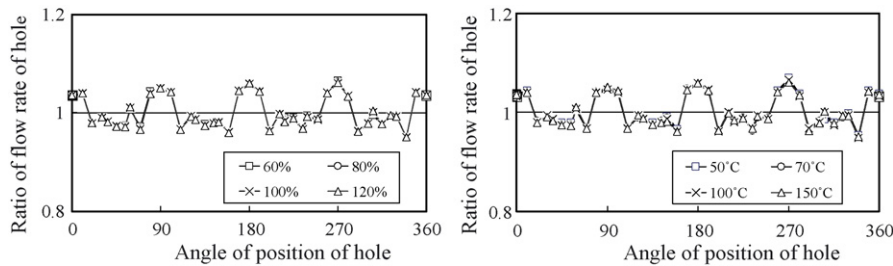


Fig. 13. Flow distribution of holes of the lower core plate.

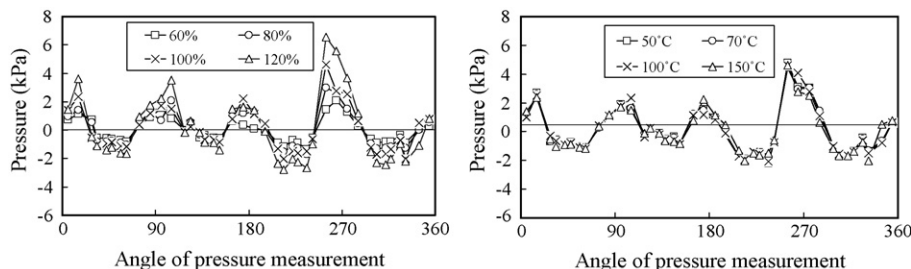


Fig. 14. Pressure distribution on the lower core plate.

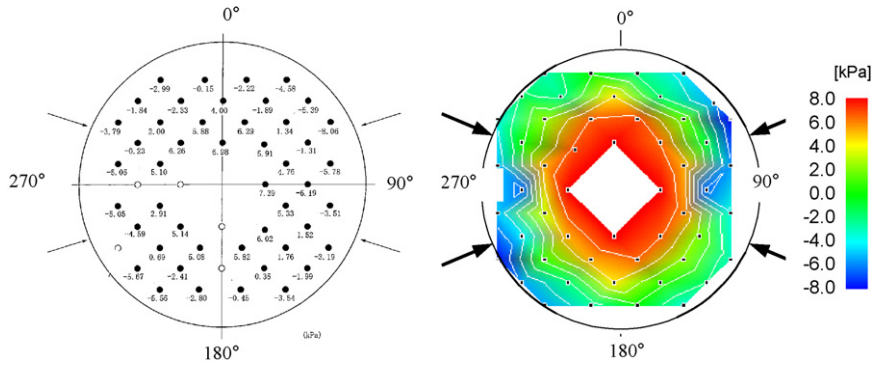


Fig. 15. Pressure distribution on the vessel bottom (100% flow, 150 °C).

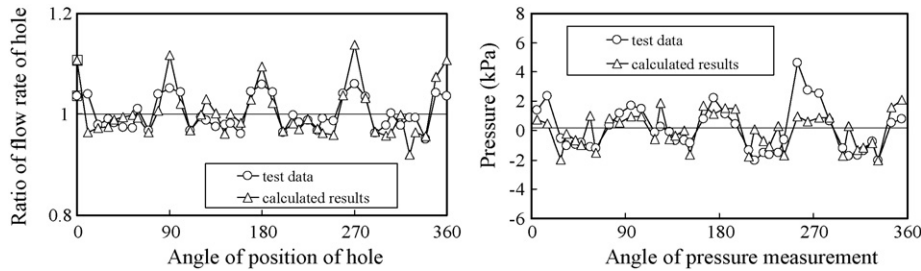


Fig. 16. Comparison test data with calculated results of the CFD code (100% flow, 150 °C).

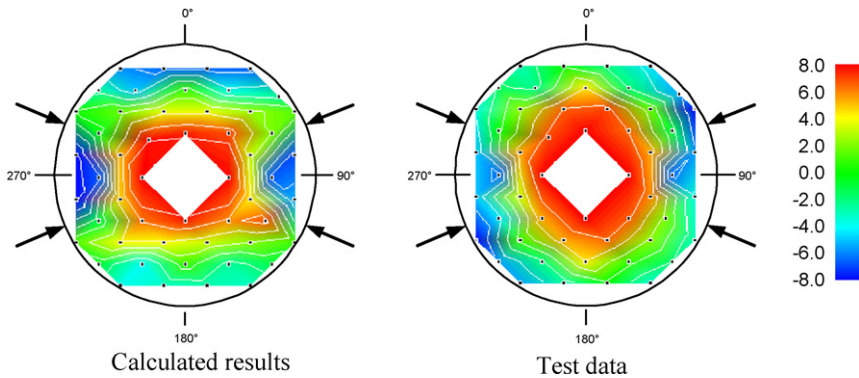


Fig. 17. Comparison test data with calculated results of the CFD code (100% flow, 150 °C).

dependency on coolant temperature. Fig. 15 shows the measured pressure on the surface of the vessel bottom that also means a deviation from the averaged pressure. The measured pressure is high in outer region where velocity along a surface is large and low in a center where velocity turns upward. Relatively low pressure can be seen in directions of 90° and 270° corresponding to a confluence of two inlet flows.

3.3. CFD calculation (Kasahara et al., 2002)

The UFLOW code (Morii et al., 2001b) calculated a 3D steady turbulent flow in the whole test vessel modelled using about 700,000 unstructured cells. The calculation was performed with the $k-\epsilon$ turbulent model and a first-order upwind method. Figs. 16 and 17 show good agreement between test data and calculated results.

4. Conclusions

A large part of data of the hydraulic flow test conducted by NUPEC from 1998 to 2002 can be utilized for CFD validation, specifically in the area of Nuclear Reactor Safety (NRS). These data are especially suitable for validating empirical models contained in the CFD codes for simulating turbulence and separate into the two groups. One is the flow induced vibration measurements utilized for validating the specific turbulent model to be able to calculate a spectrum of pressure fluctuation such as the LES model and the other is the flow distribution measurements for the general turbulent model, for example, the $k-\epsilon$ turbulent model. Boundary shapes of the former flow field are relatively simple, but the latter involve the specific shapes of plates in the lower plenum and inlet holes of the radial neutron reflector peculiar to the Japanese APWR design. Therefore,

it is important for using the data of the flow distribution measurements to validate the CFD code that these boundary shapes should be exactly reflected in the calculation grid of the CFD code.

Histories of pressure fluctuation of the coolant in the several locations of the downcomer were obtained by the flow induced vibration measurements and rearranged into several data by the statistical process. These data can be classified as follows depending on the level of capability of the turbulent model validated by them:

- *Level 1.* Total pressure fluctuations (integral of frequency).
- *Level 2.* Spectrum of pressure fluctuations.
- *Level 3.* Correlation between adjacent pressure fluctuations.

A correct simulation of the higher level data by the CFD code needs the more sophisticated turbulence model and the more sufficient fine grids. For example, the calculated results with the LES model and 550,000 grids agreed well with the data of the levels 1 and 2, but did not agreed very well with the level 3.

Acknowledgments

This paper represents a summarizing report on a project sponsored by the Ministry of Economy, Trade and Industry, to which many colleagues and coworkers from various institutions have contributed. These include the members of the Nuclear Power Engineering Corporation, the Mitsubishi Heavy Industries Ltd. and the Mizuho Information & Research Institute Inc.

Appendix A. Common mode noise caused by the proper vibration of piping system

The histories and spectrums of the measured pressure fluctuation at various locations in the downcomer of the test vessel are shown as gray lines in Fig. A1. Every figure but 90° of upper part of the downcomer was similar to each other in spite of measurement at different locations. In order to grasp it quantitatively, strength of correlation with the fluctuation of 0° of upper part is calculated by rearranging the measured data statistically and is shown as gray lines in Fig. A2. All but 90° of upper part correlates tight with the fluctuation of 0° of upper part in the

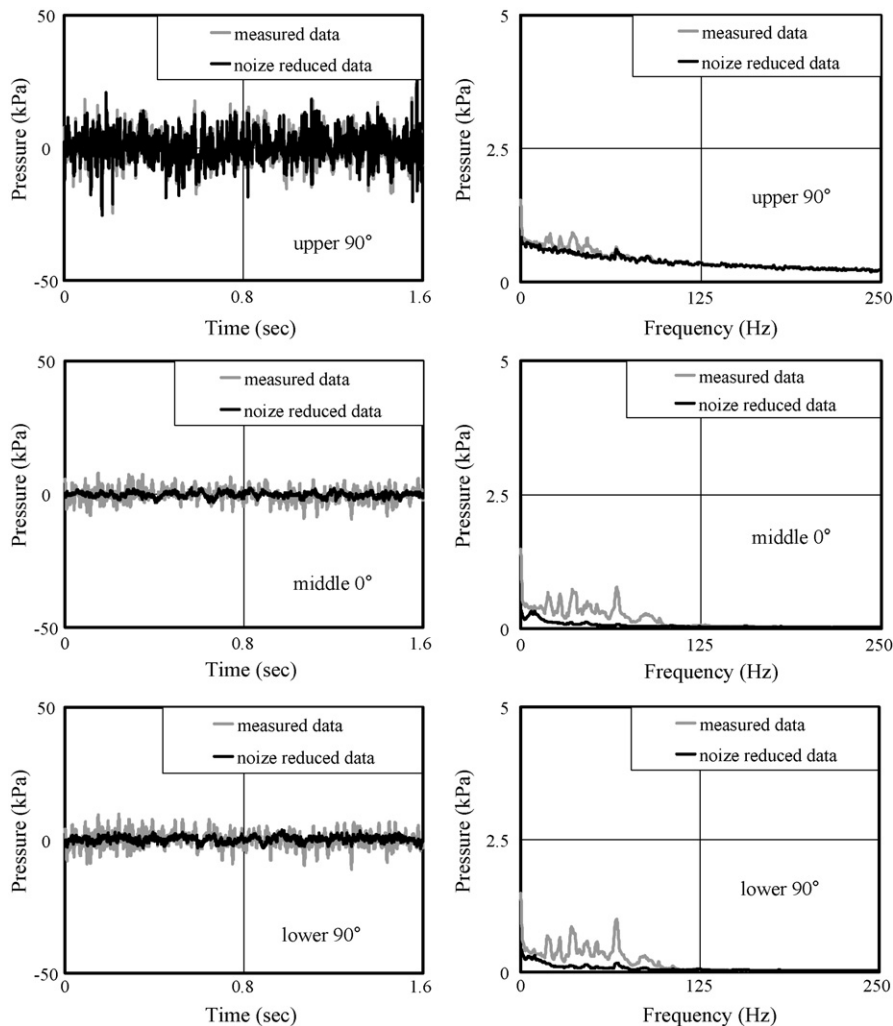


Fig. A1. Comparison of pressure fluctuations and spectrums.

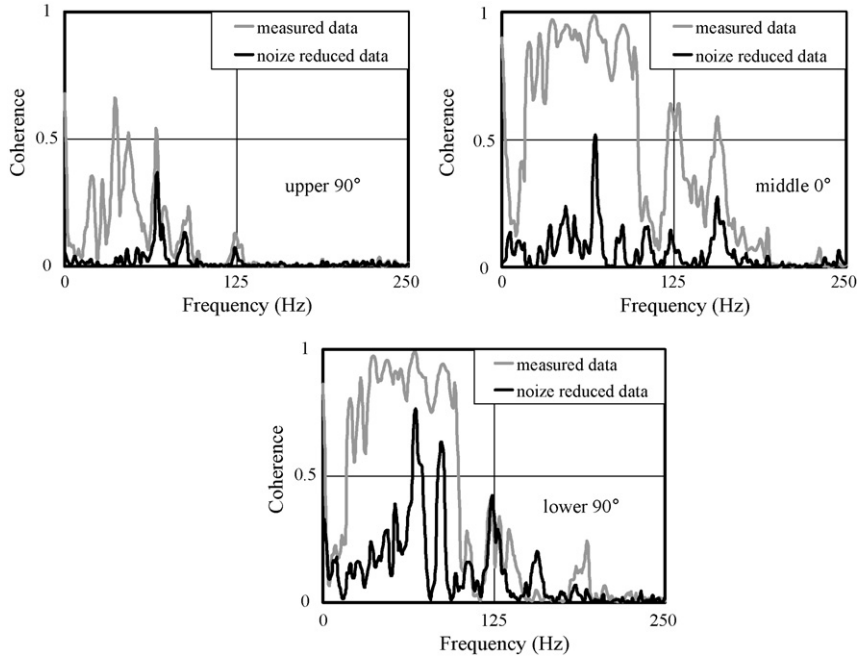


Fig. A2. Comparison of coherence with upper 0° data.

range of frequency between 20 Hz and 100 Hz. Since these correlated pressure fluctuations are common mode noise caused by the proper vibration of the piping system of the test facility and have no relation to turbulence, it is necessary for CFD code validation to separate and subtract its component from the measured fluctuations.

A.1. Process of common mode noise reduction

The measured pressure of the i th pressure transducer p_i is assumed to be summation of the common mode noise p_0 and random fluctuation of turbulence p'_i :

$$p_i = p_0 + p'_i \tag{A1}$$

The random fluctuation p'_i near the inlet nozzle such as 90° of upper part is considered to be larger than the noise level p_0 and at the other locations, p'_i smaller than p_0 . The approximate value of the common mode noise \bar{p}_0 is estimated to average p_i of every location but neighborhood of the inlet nozzle:

$$\bar{p}_0 = \frac{\sum_i p_i}{n} = p_0 + \frac{\sum_i p'_i}{n} \tag{A2}$$

Difference between \bar{p}_0 and p_0 reduces as the number of averaged pressure n increases because $\sum_i p'_i/n$ approaches 0. Then, we can estimate the random turbulence pressure p'_i by subtracting \bar{p}_0 from measured data as the following equation:

$$p'_i \approx p_i - \bar{p}_0 = p_i - \frac{\sum_i p_i}{n} \tag{A3}$$

Bold lines in Figs. A1 and A2 show the histories, spectrums and coherence levels of the pressure fluctuation after noise reduction compared with the measured data. It can be seen from these figures that some peaks of spectrum corresponding to the

proper vibration of piping system disappear and coherence level decreases as expected.

A.2. Remedying process to obtain the power spectrum of turbulence

Fig. A3 shows the normalized power spectrums of the pressure fluctuation measured at the representative locations in the downcomer. It is well-known by the Kolmogorv theory that turbulent energy in an inertia region decrease by the $-5/3$ power of a frequency. Since a power spectrum of pressure fluctuation is proportional to turbulent energy, a line of the $-5/3$ power of a frequency is able to be included in Fig. A3. The normalized power of fluctuation near the inlet nozzle of upper 45°, 90° and 135° decreases according to the law of the $-5/3$ power beyond one non-dimensional frequency (24 Hz). The other spectrums, by contrast, are swollen with some peaks in the range from 1 to 5 (120 Hz) of non-dimensional frequency and decreases according to the law of the $-5/3$ power beyond 5. This swelling that is caused by the proper vibration of piping system of the test

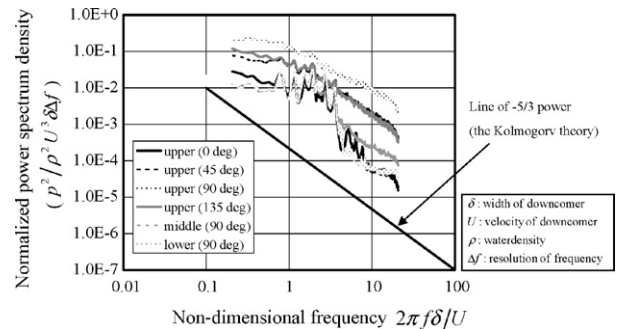


Fig. A3. The normalized power spectrums of the measured pressure fluctuation.

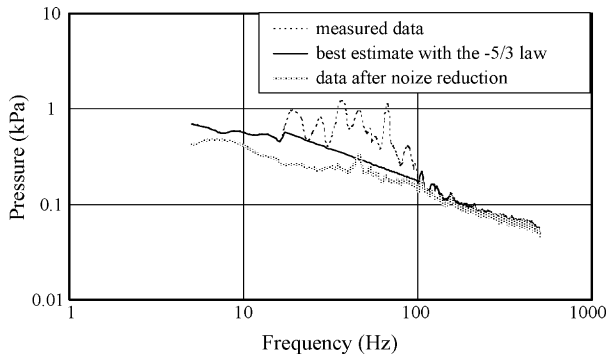


Fig. A4. Subtraction of a component due to the proper vibration of piping system.

facility is subtracted from the measured spectrums as shown in Fig. A4. Fig. A4 also include the spectrum obtained by the noise reduction process mentioned previously. It can be seen from the figure that the noise reduction process succeeds in subtracting

an effect by the proper vibration of the facility, but results in underestimating pressure level.

References

- Au-Yang, M.K., 1980. Dynamic pressure inside a PWR—a study based on laboratory and field test data. *Nucl. Eng. Des.* 58, 113–125.
- Au-Yang, M.K., 1999. Common mistakes and misconceptions in flow-induced vibration and coupled fluid-structural dynamics analysis. In: *ASME International Tutorial at PVP Conference*.
- Gavrilas, M., et al., November 2000. OECD/CSNI ISP No. 43 Rapid Boron-dilution Transient Tests for Code Verification, NEA/CSNI/R(2000)22.
- Kasahara, F., et al., 2002. Improvement of hydraulic flow analysis code for APWR reactor internals. In: *CFD Meeting Presentation Material in Aix en Provence, May*.
- Morii, T., et al., 2001a. Hydraulic behavior test and analysis of APWR for safety analysis codes (in Japanese). In: *Proceedings of the Meeting of the Atomic Energy Society of Japan, Sapporo, September*.
- Morii, T., et al., 2001b. Benchmark analysis of rapid boron dilution transient by the PLASHY/IMPACT code. In: *Proceedings of the 8th International Symposium on Flow Modeling and Turbulence Measurements, Tokyo, December*.